



Extreme conditions during multibubble cavitation: Sonoluminescence as a spectroscopic probe

Kenneth S. Suslick*, Nathan C. Eddingsaas, David J. Flannigan, Stephen D. Hopkins, Hangxun Xu

Department of Chemistry, University of Illinois at Urbana-Champaign, 600 South Mathews Avenue, Urbana, IL 61801, USA

ARTICLE INFO

Article history:

Received 5 October 2010

Received in revised form 8 December 2010

Accepted 23 December 2010

Available online 31 December 2010

Keywords:

Sonoluminescence
Emission temperature
Cavitation
MBSL
Plasma

ABSTRACT

We review recent work on the use of sonoluminescence (SL) to probe spectroscopically the conditions created during cavitation, both in clouds of collapsing bubbles (multibubble sonoluminescence, (MBSL)) and in single bubble events. The effective MBSL temperature can be controlled by the vapor pressure of the liquid or the thermal conductivity of the dissolved gas over a range from ~ 1600 to ~ 9000 K. The effective pressure during MBSL is ~ 300 bar, based on atomic line shifts. Given nanosecond emission times, this means that cooling rates are $>10^{12}$ K/s. In sulfuric and phosphoric acid, the low volatility and high solubility of any sonolysis products make bubble collapse more efficient and evidence for an optically opaque plasma core is found.

© 2011 Elsevier B.V. All rights reserved.

1. Introduction

No direct coupling of the acoustic field with chemical species on a molecular level can account for sonochemistry [1–10] or sonoluminescence (SL) [11–18]. Ultrasound spans the frequencies of roughly 15 kHz–10 MHz, with associated acoustic wavelengths in liquids of roughly 100–0.1 mm: these are not on the scale of molecular dimensions. Instead, the chemical effects of ultrasound derive from several non-linear acoustic phenomena, of which cavitation is the most important. Ultrasound can induce unique high-energy chemistry through this process of acoustic cavitation [19–23]: the formation, growth, and implosive collapse of bubbles in a liquid, which can create extreme conditions in localized, short-lived hot spots. During the past few years, we have begun to develop a detailed picture of the nature of cavitation collapse and its chemical effects primarily through spectroscopic studies of SL, both from clouds of cavitating bubbles (multibubble sonoluminescence (MBSL), Fig. 1) and from single isolated cavitating bubbles (Single Bubble Sonoluminescence (SBSL)). Herein we will review our experimentally determined understanding of the conditions created in clouds of collapsing bubbles.

Acoustic cavitation in a liquid irradiated with ultrasound can be quantitatively described with excellent accuracy throughout nearly all of the process of formation, growth, and compression by modeling the radial motion of an acoustically driven bubble with any of a family of equations related to the Rayleigh-Plesset

equation (RPE). RPEs can vary in complexity and have been built up with contributions by many researchers over the past century [19–23]. An example of an RPE is shown in Eq. (1).

$$R\ddot{R} + \frac{3}{2}\dot{R}^2 = \frac{1}{\rho} \left[\left(P_0 + \frac{2\sigma}{R_0} \right) \left(\frac{R_0}{R} \right)^{3\gamma} - \frac{2\sigma}{R} - \frac{4\mu\dot{R}}{R} + P_\infty \right] \quad (1)$$

Here, R is the bubble radius (with the overdots signifying first (velocity) and second (acceleration) derivatives of the interface with respect to time), R_0 is the bubble radius at ambient conditions, ρ is the bulk liquid density, P_0 is the ambient liquid pressure, σ is the surface tension, μ is the shear viscosity, and P_∞ is the far-field acoustic pressure. The left side of Eq. (1) describes the inertial characteristics of the bubble interface. The first term on the right side represents the intracavity gas pressure as the bubble radius varies from R_0 to R . RPEs work very well over most of the range of bubble motion, as shown qualitatively in Fig. 2; any RPE assumes, however, that the density of the liquid is very large compared to the density of the gas within the bubble. This assumption fails in the case of a strongly driven bubble as it rapidly approaches its minimum radius. So it is only in the last stage of collapse does theoretical description of the implosive collapse of bubbles become problematic, but of course everything of interest occurs only in the last stage of collapse!

2. MBSL and conditions in bubble clouds

The light emitted by SL potentially provides a spectroscopic probe of the conditions created within collapsing bubbles [11].

* Corresponding author. Tel.: +1 217 333 2794.

E-mail address: ksuslick@uiuc.edu (K.S. Suslick).



Fig. 1. MBSL. A photo of a MBSL cloud from an ultrasonic horn (1 cm diameter) in 95 wt.% H_2SO_4 under Xe is shown.

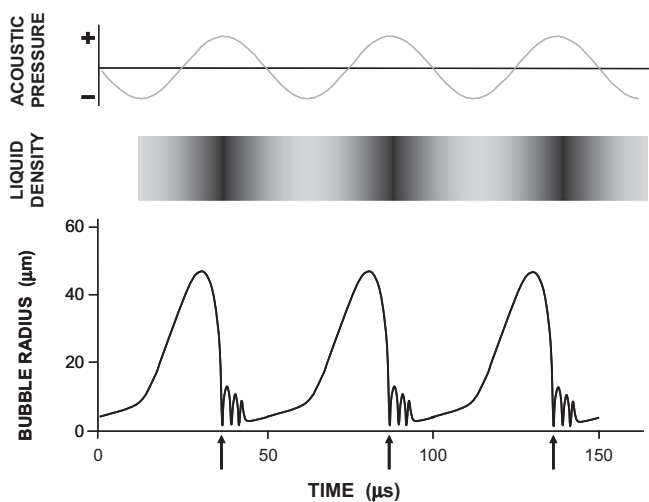


Fig. 2. Bubble growth and collapse during single bubble cavitation at 20 kHz. The origin of sonochemistry and SL occurs (as indicated by the arrows) at the point of maximum bubble compression.

By comparing the relative intensities of emission lines from electronically excited atoms and molecules, an effective “emission temperature” can be determined if one already knows the intrinsic emissivity of observed emission lines [11]. This same technique was developed long ago to quantify the thermal conditions of high-temperature sources (e.g., plasmas and flames) and remote locations (e.g., stellar surfaces). The observation of discrete emission lines is of course a prerequisite for such an approach. MBSL spectra typically contain emission lines and so are quite amenable to this technique. By examining the relative intensity of two or more emission lines, one may calculate the expected relative intensities as a function of effective temperature. One should note in contrast that other spectrometric methods of pyrometry that make use of continuous radiative transitions rather than discrete transitions are highly model dependent (i.e., is the emission due to blackbody or bremsstrahlung or line broadened molecular emission, etc.).

Our group was the first to measure the temperatures and pressures created during acoustic cavitation [4,24], using spectroscopic

thermometry from atomic and molecular emission of SL both in multibubble clouds [25–37] and in single bubbles [38–48]. Both metal atom emission and molecular emission bands can be used to probe the temperatures formed during MBSL. For example, the emission lines observed from chromium atom excited states (i.e., Cr^*) during the sonication of a solution of $\text{Cr}(\text{CO})_6$ dissolved in silicone oil under Ar at 20 kHz are shown in Fig. 3. By using the two-line radiance ratio method and comparing the MBSL emission to simulated emission spectra at various temperatures, the effective MBSL temperature was found to be 4700 ± 300 K. Using the same method for other metal carbonyls also produced temperatures of ~ 5000 K: Fe gave 5100 ± 300 K, and Mo 4800 ± 400 K. MBSL temperatures determined in this manner compare very well to the emission temperature of 5100 ± 200 K determined by simulating the C_2 emission bands observed during sonication of low volatility *n*-alkanes [24].

One may also use MBSL to determine the intracavity pressures generated during cavitation by again using emission lines from electronically-excited atoms. Rather than using the line-intensities (as for temperature determinations), instead peak shifts are used to determine pressures. Perturbations of the energy levels of radiating species as well as reductions in the excited-state lifetimes due to an increase in the collisional frequency with other species leads to shifts in peak positions and broadening of line profiles (i.e., Uncertainty Principle broadening). By quantifying the various factors that lead to changes in line positions and profiles (e.g., Doppler effects, instrument contributions, pressure broadening, etc.), an overall pressure at some specific temperature can be determined. Note that in a plasma (as we shall find for SBSL), the contribution to the line profile from Stark effects and (to a lesser extent) ion broadening must also be considered.

As an example, our group measured experimentally the pressures generated during MBSL by quantifying the peak shifts in the emission lines from Cr^* during the sonication of solutions of silicone oil saturated with He or Ar and containing $\text{Cr}(\text{CO})_6$ [28]. Line shifts were found to be more reliable for pressure determinations than line widths because of the artificial line broadening created by light scattering off the bubble cloud. Theory on the behavior of the peak positions of emission lines of transition metal atoms has not yet advanced to the point that pressures can be determined in this manner a priori. Quantitative determinations can, however, be made by comparison of MBSL emission line positions to those observed from ballistic compressors, the conditions within which approximate the conditions during acoustic cavitation. Because reliable high-pressure data for Cr^* emission lines exists in the literature [49], pressure estimates can be made directly from MBSL Cr^* emission lines, as shown in Fig. 4. By comparing the observed shift of the MBSL Cr^* lines to ballistic compressor data and extrapolating to temperatures observed during cavitation (4700 K), pressures of 300 ± 30 bar were determined [28]. Because the ballistic compressor data showed that the degree of Cr^* line red shift decreased with increasing temperature, the pressure of 300 bar was taken as a lower limit.

3. Conditions during MBSL in ionic liquids

Most prior MBSL studies so far discussed were in low vapor pressure alkanes or silicone oils. The importance of low vapor pressure liquids lies in both the heat capacity ratio ($\gamma = C_p/C_v$, which determines the temperature from compression of a gas) and from the endothermic sonolysis of gas molecules found inside collapsing bubbles: if there are high concentrations of vapor, the effect of the bubble compression is lost and substantial heating does not occur. Furthermore, if sonolysis of the liquid produces volatile polyatomic species, one faces eventually the same problems. Liquids that have

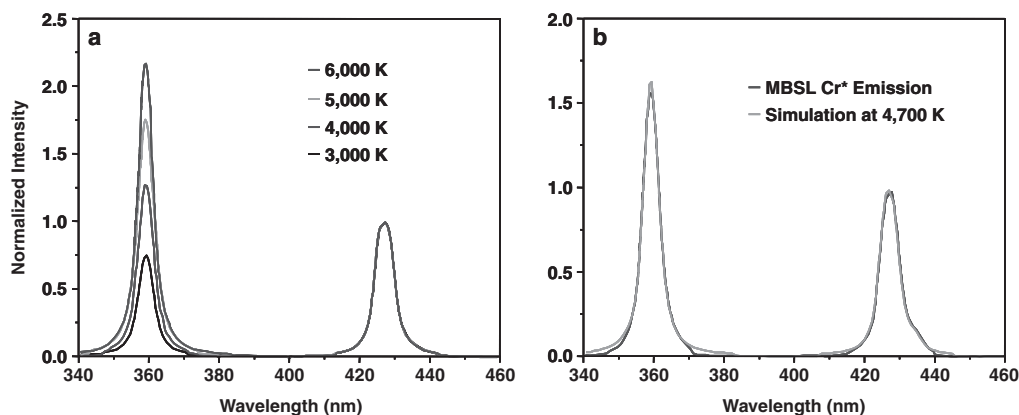


Fig. 3. (a) Simulations of thermally equilibrated emission from Cr^* atoms. The simulated spectra have been normalized to the peak intensity of the convoluted triplet at 424 nm. (b) MBSL from a solution of $\text{Cr}(\text{CO})_6$ in silicone oil saturated with Ar gas, compared to a simulation at 4700 K. The underlying continuum was subtracted from the MBSL spectrum for clarity [11].

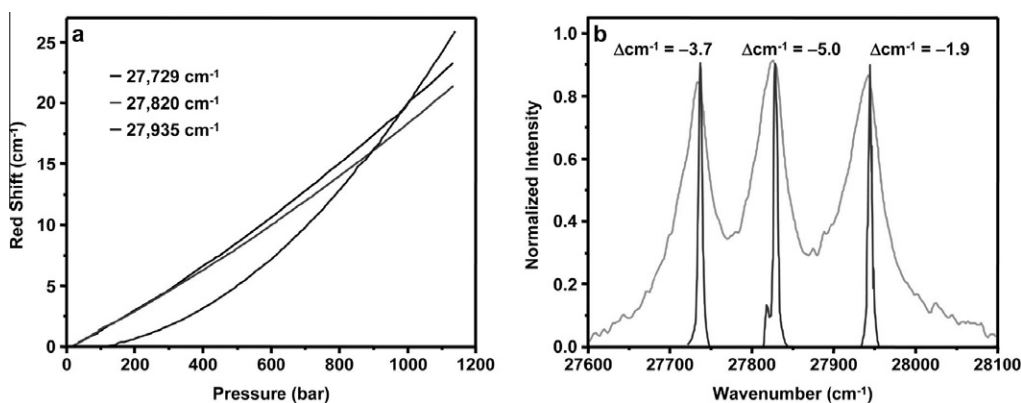


Fig. 4. (a) Dependence of the peak positions of emission lines of Cr^* atoms on the pressure of a bath gas of Ar at a temperature of 3230 K. The wavenumber labels indicate the peak positions of the Cr^* emission lines under ambient conditions. (b) Comparison of the MBSL Cr^* emission lines (gray, relatively broad) to the Cr^* emission lines from a low pressure hollow cathode lamp (black, relatively narrow). Each MBSL Cr^* line is labeled with its energy shift (red-shift) relative to the hollow cathode lamp lines [11].

both a low vapor pressure and highly soluble sonolysis products are therefore preferred for the generation of higher temperatures during cavitation. We have recently extended our SL studies to other low volatility liquids [35–37], most notably sulfuric and

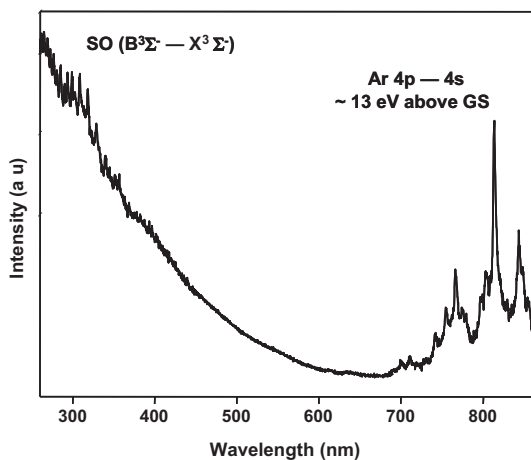


Fig. 5. Spectrum of MBSL from concentrated sulfuric acid sparged with Ar. The spectrum consists of a broad continuum extending into the UV with SO and Ar lines on top. Temperature measurements using the Ar lines yields a temperature around 8000 K [35].

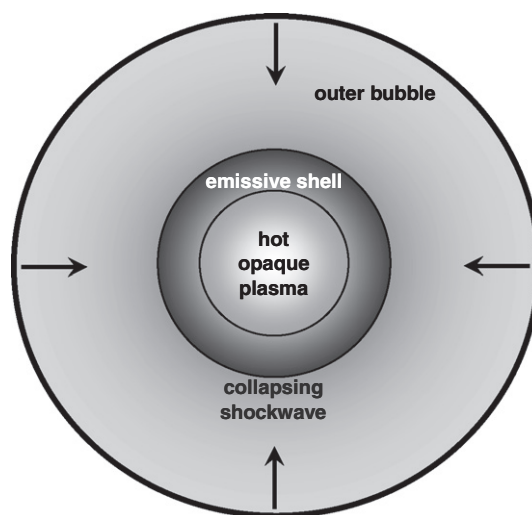


Fig. 6. As a bubble collapse occurs, under some specific conditions (e.g., in very low vapor pressure liquids such as concentrated sulfuric acid), it appears that a spherical shockwave may be launched. An optically opaque plasma core is formed as that shockwave converges, and escaping energetic electrons together with the compressional heating of the collapse are responsible for the emission observed during SBSL in sulfuric acid [35]. The emissive shell is analogous to the photosphere of a star and the plasma's opacity hides any optical information from the opaque interior core.

phosphoric acid, the latter of which has proved exceptionally versatile. Of special interest here, phosphoric acid does not boil or truly decompose: it simply dehydrates, reversibly releasing water, so that under sonolysis, no long-term production of volatiles (and consequent poisoning of the bubble interior with polyatomics) occurs.

In both sulfuric and phosphoric acid, we were able to generate MBSL with exceptionally high intensity, indeed easily observable by the naked eye, even in a well-lit room. In sulfuric acid under Ar, we were surprised to see atomic emission from the Ar 4p–4s system, as shown in Fig. 5 [35]. Effective emission temperatures can be determined from the observed Ar lines, and we found an effective temperature of ~ 8000 K at 20 kHz (14 W/cm^2) with a Ti horn directly immersed in 95 wt.% sulfuric acid sparged with Ar, ~ 298 K. Interestingly, at this temperature, there would *not* be any appreciable number of Ar atoms thermally excited into the 4p state (which ~ 13 eV above the ground state). This apparent paradox indicates that, as we will discuss shortly for SBSL, a optically opaque plasma [50–51] is probably formed at the core of the collapsing bubble in sulfuric acid, and that the Ar emission results from collision excitation with higher energy electrons [35]. With any significant ionization, a plasma becomes opaque to light and so emission no longer comes from the plasma core, but only from an emissive shell on the outer edge of the ionization, in exact analogy to the photosphere of a star [50], as illustrated in Fig. 6. The presence of a plasma during MBSL has been postulated numerous times [52–54], but this remains the only experimental evidence. In contrast, however, it is now well established that a plasma is formed during SBSL, as evidenced by direct observation of various ions (O_2^+ , Xe^+ , Kr^+ , Ar^+) with energies as high as 37 eV above ground state [40–42,47–48].

MBSL from phosphoric acid [37] makes for an interesting comparison to sulfuric acid. H_3PO_4 is a strongly hydrogen-bonded liquid; it too has a relatively high viscosity and low vapor pressure (~ 2.4 torr for 85% H_3PO_4). Interestingly, the vapor of H_3PO_4 consists of water molecules alone; there are no acid molecules present in the vapor over most concentrated H_3PO_4 even at high temperatures. Thus, in the gas phase of H_3PO_4 , the only volatile component inside the bubbles is water vapor; the phosphoric acid molecules can be considered as nonvolatile species during MBSL. The origin of the MBSL from 85% H_3PO_4 emission depends on the dissolved inert gas. Under He or Ne, the MBSL spectra show strong molecular emission from OH ($A^2\Sigma^+-X^2\Pi$) and PO β system ($B^2\Sigma^+-X^2\Pi$), with

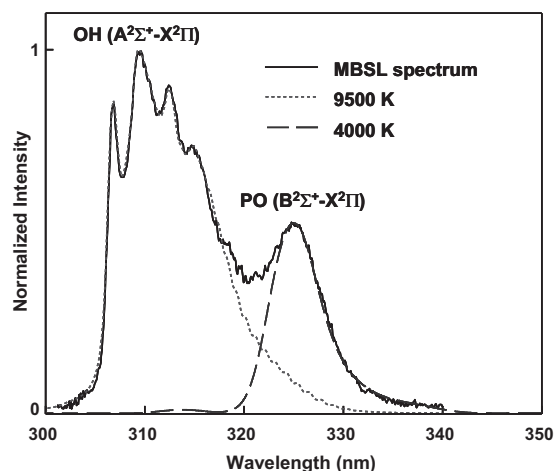


Fig. 7. Spectrum of OH ($A^2\Sigma^+-X^2\Pi$) and PO ($B^2\Sigma^+-X^2\Pi$) emission from MBSL in 85% H_3PO_4 saturated with He and irradiated with ultrasound compared to the best fit calculated spectra (dotted line: calculated OH emission spectrum at 9500 K; dashed line: calculated PO emission spectrum at 4000 K) [37].

bands at 310 and 325 nm, respectively (Fig. 7). The OH and PO molecular emission bands are monotonically broadened as the dissolved gas goes from He to Ne to Ar to Kr to Xe, until the molecular emission bands are broadened completely. Given the higher expected cavitation temperatures with the heavier noble gases (due to decreased thermal conductivity), the broadening of the molecular emission is consistent with expected dissociation of the OH and PO radicals.

With phosphoric acid MBSL, one has the unique situation of two different spectroscopic thermometers in the same cavitation event: temperatures can be calculated for both OH and PO molecular emission [37]. Calculated OH emission spectra can be generated easily, and fitting our experimental spectra for OH emission with calculated spectra yields an effective emission temperature of 9500 ± 300 K. The emission from excited PO radicals can also be used as a spectroscopic thermometer to probe the intracavity temperatures generated during MBSL. The β system of PO emission in the 320–340 nm wavelength range has been extensively studied. By fitting the PO emission spectra (Fig. 7), the emission temperature of PO is determined to be 4000 ± 400 K, which is *substantially lower* than that measured from OH emission (9500 ± 300 K).

At first glance, the different MBSL temperatures from the two simultaneously-observed, independent molecular species are paradoxical because both OH and PO emissions are from same cavitation event. The observed temperature inhomogeneity, however, can be explained by the two different cavitating bubble populations involving nonvolatile species. We recently demonstrated [36] by doping H_3PO_4 with Na_3PO_4 that there are two distinct cavitating bubble populations in H_3PO_4 : (1) stationary bubbles whose collapse is highly symmetric and (2) rapidly moving bubbles whose collapse is much less symmetric and associated injection of liquid nanodroplets into the gas phase of the collapsing bubbles. The OH emission comes dominantly from the first class of collapsing bubbles. In contrast, the PO radical, which is a decomposition product from nonvolatile H_3PO_4 molecules, is analogous to the emission of alkali metal atoms in aqueous solution and represents the conditions present in the second class of cavitating bubbles.

Indeed, consistent with this interpretation, we also observe spatial separation of the cavitating bubble populations. With an ultrasonic horn, there are two different bubble populations: OH emission appears both at the top and bottom of the cavitating bubble cloud, whereas PO emission is only observable at the bottom of the cloud, further away from the ultrasonic horn. The emission of PO radicals comes from non-volatiles and involves injection of liquid droplets into the interior of bubbles via capillary wave action, microjetting or bubble coalescence due to the significant deformation during bubble collapse in the dense cloud of cavitating bubbles. Once the droplets enter the hot interior of the bubble, the solvent evaporates and decomposition of H_3PO_4 molecules analogous to the processes in flames begins which generates excited PO radicals. The evaporation of the solvent in the liquid droplet and endothermic decomposition of H_3PO_4 and H_2O molecules consume a great amount of cavitation energy. Thus liquid droplets can cool down hot spots inside the cavitating bubbles which contain liquid droplets. The measured PO emission temperature represents

Table 1
Conditions during MBSL.

Temperature	~ 1600 to 9500 K (vapor pressure controlled)
Pressure	~ 300 bar
Plasma density	generally $\sim 0 \text{ cm}^{-3}$
Duration	~ 1 ns
Cooling rate	$> 10^{12}$ K/s

the hot spot conditions inside nonsymmetrically collapsing bubbles that contain liquid droplets and is much lower than the measured OH emission temperature that dominantly represents the more symmetric collapsing bubbles. Presumably, the spatial separation of the two bubble populations is caused by the pressure gradient propagated from the ultrasonic horn; one might not observe such separation in a more uniform ultrasonic field.

4. Conclusions

Spectroscopic methods have become a formidable method of quantifying the temperatures and pressures generated during cavitation in clouds of collapsing bubbles, as summarized in Table 1. MBSL has provided a quantitative measure of the emission temperature from a wide range of liquids (from silicone oils to alkanes to concentrated acids), using a variety of reporting emitters (including noble gas and metal atoms, C₂, OH, and PO). Control over the effective temperature inside the bubbles is dominated by the vapor pressure of volatiles present in the liquid and secondarily by the thermal conductivity of dissolved gas. The pressure felt by the emitting species has also been measured by use of atomic line shifts. Finally, MBSL provides a spatial probe of the different bubble populations present in dense cavitation clouds; in general we find that there are two distinct cavitating bubble populations: (1) bubbles near the acoustic horn whose collapse is highly symmetric and whose emission temperatures are hotter and (2) rapidly moving cooler bubbles whose collapse is much less symmetric and associated injection of liquid nanodroplets into the gas phase of the collapsing bubbles.

Acknowledgments

We dedicate this paper to the memory of Oleg Abramov, a great bear of a man, whose good fellowship and thoughtful approach to science we sorely miss. In 1994, Oleg and his daughter spent an extended stay in our labs in Urbana, which was a highpoint of our sonochemical research. We gratefully acknowledge the financial support of the U.S. National Science Foundation (CHE and DMR).

References

- [1] S. Suslick (Ed.), *Ultrasound, Its Chemical, Physical, and Biological Effects*, VCH Publishers, New York, 1988.
- [2] T.J. Mason, J.P. Lorimer, *Applied Sonochemistry: Uses of Power Ultrasound in Chemistry and Processing*, Wiley-VCH, Weinheim, 2002.
- [3] L.A. Crum, T.J. Mason, J. Reisse, K.S. Suslick (Eds.), *Sonochemistry and Sonoluminescence*, Kluwer Publishers, Dordrecht, Netherlands, 1999, NATO ASI Series C, vol. 524.
- [4] K.S. Suslick, *Science* 247 (1990) 1439.
- [5] K.S. Suslick, *Sci. Am.* 260 (1989) 80.
- [6] Pankaj, M. Ashokkumar (Eds.), *Theoretical and Experimental Sonochemistry Involving Inorganic Systems*, Springer, New York, 2011.
- [7] K.S. Suslick, Y.T. Didenko, M.M. Fang, T. Hyeon, K.J. Kolbeck, W.B. McNamara III, M.M. Mdeleeni, M. Wong, *Phil. Trans. Roy. Soc. London A* 357 (1999) 335.
- [8] G. Cravotto, P. Cintas, *Chem. Soc. Rev.* 35 (2006) 180.
- [9] J.H. Bang, K.S. Suslick, *Adv. Mater.* 22 (2010) 1039.
- [10] K.S. Suslick, G. Price, *Annu. Rev. Mater. Sci.* 29 (1999) 295.
- [11] K.S. Suslick, D.J. Flannigan, *Annu. Rev. Phys. Chem.* 59 (2008) 659.
- [12] D.F. Gaitan, L.A. Crum, C.C. Church, R.A. Roy, *J. Acoust. Soc. Am.* 91 (1992) 3166.
- [13] B.P. Barber, R.A. Hiller, R. Lofstedt, S.J. Putterman, K.R. Weninger, *Phys. Rep.* 281 (1997) 66.
- [14] S.J. Putterman, K.R. Weninger, *Annu. Rev. Fluid Mech.* 32 (2000) 445.
- [15] M.P. Brenner, S. Hilgenfeldt, D. Lohse, *Rev. Mod. Phys.* 74 (2002) 425.
- [16] K. Yasui, T. Tuziuti, M. Sivakumar, Y. Iida, *Appl. Spectrosc. Rev.* 39 (2004) 399.
- [17] S. Hilgenfeldt, *Nat. Phys.* 2 (2006) 435.
- [18] M. Ashokkumar, F. Grieser, *ChemPhysChem* 5 (2004) 439.
- [19] T.G. Leighton, *The Acoustic Bubble*, Academic Press, London, 1994.
- [20] F.R. Young, *Cavitation*, Imperial College Press, London, 1999.
- [21] C.E. Brennen, *Cavitation and Bubble Dynamics*, Oxford University Press, New York, 1995.
- [22] K.S. Suslick, T.J. Matula, *Acoustic Cavitation, Sonochemistry, and Sonoluminescence*, in: J.G. Webster (Ed.), *Wiley Encyclopedia of Electrical and Electronics Engineering*, vol. 22, Wiley-Interscience, New York, 1999, pp. 646–657.
- [23] D. Lohse, *Phys. Today* 56 (2003) 36.
- [24] E.B. Flint, K.S. Suslick, *Science* 253 (1991) 1397.
- [25] L.S. Bernstein, M.R. Zakin, E.B. Flint, K.S. Suslick, *J. Phys. Chem.* 100 (1996) 6612.
- [26] W.B. McNamara III, Y.T. Didenko, K.S. Suslick, *Nature* 401 (1999) 772.
- [27] W.B. McNamara III, Y.T. Didenko, K.S. Suslick, *Phys. Rev. Lett.* 84 (2000) 777.
- [28] W.B. McNamara III, Y.T. Didenko, K.S. Suslick, *J. Phys. Chem. B* 107 (2003) 73036.
- [29] K.S. Suslick, E.B. Flint, *Nature* 330 (1987) 553.
- [30] E.B. Flint, K.S. Suslick, *J. Am. Chem. Soc.* 111 (1989) 6987.
- [31] K.S. Suslick, E.B. Flint, M.W. Grinstaff, K.A. Kemper, *J. Phys. Chem.* 97 (1993) 3098.
- [32] W.B. McNamara III, Y.T. Didenko, K.S. Suslick, *J. Am. Chem. Soc.* 121 (1999) 5817.
- [33] Y.T. Didenko, W.B. McNamara III, K.S. Suslick, *J. Phys. Chem. A* 103 (1999) 10783.
- [34] W.B. McNamara III, Y.T. Didenko, K.S. Suslick, *J. Am. Chem. Soc.* 122 (2000) 8563.
- [35] N.C. Eddingsaas, K.S. Suslick, *J. Am. Chem. Soc.* 129 (2007) 3838.
- [36] H.X. Xu, N.C. Eddingsaas, K.S. Suslick, *J. Am. Chem. Soc.* 131 (2009) 6060.
- [37] H.X. Xu, N.G. Glumac, K.S. Suslick, *Angew. Chem. Int. Ed.* 48 (2010) 1079.
- [38] Y.T. Didenko, K.S. Suslick, *Nature* 418 (2002) 394.
- [39] Y.T. Didenko, W.B. McNamara III, K.S. Suslick, *Nature* 406 (2000) 877.
- [40] D.J. Flannigan, K.S. Suslick, *Nature* 434 (2005) 52.
- [41] D.J. Flannigan, K.S. Suslick, *Phys. Rev. Lett.* 95 (2005) 044301.
- [42] D.J. Flannigan, K.S. Suslick, *Acoust. Res. Lett. Online* 5 (2005) 157.
- [43] S.D. Hopkins, S.J. Putterman, B.A. Kappus, K.S. Suslick, C.G. Camara, *Phys. Rev. Lett.* 95 (2005) 254301.
- [44] D.J. Flannigan, K.S. Suslick, *J. Phys. Chem. A* 110 (2006) 9315.
- [45] D.J. Flannigan, K.S. Suslick, *Phys. Rev. Lett.* 99 (2007) 134301.
- [46] C.G. Camara, S.D. Hopkins, K.S. Suslick, S.J. Putterman, *Phys. Rev. Lett.* 98 (2007) 064301.
- [47] H.X. Xu, K.S. Suslick, *Phys. Rev. Lett.* 104 (2010) 244301.
- [48] D.J. Flannigan, K.S. Suslick, *Nat. Phys.* 6 (2010) 598.
- [49] Q.A. Holmes, M. Takeo, S.Y. Ch'en, *J. Quant. Spectrosc. Radiat. Transfer* 9 (1969) 761.
- [50] Y.B. Zel'dovich, Y.P. Raizer, *Physics of Shock Waves and High-Temperature Hydrodynamic Phenomena*, Academic Press, New York, 1966.
- [51] W.C. Moss, D.A. Young, J.A. Harte, J.L. Levatin, B.F. Rozsnyai, G.B. Zimmerman, I.H. Zimmerman, *Phys. Rev. E* 59 (1999) 2986.
- [52] Y.T. Didenko, T.V. Gordeychuk, *Phys. Rev. Lett.* 84 (2000) 5640.
- [53] K. Yasui, *J. Chem. Phys.* 115 (2001) 2893.
- [54] K.R. Weninger, C.G. Camara, S.J. Putterman, *J. Phys. Rev. E: Stat. Phys. Plasmas Fluids Relat. Interdiscip. Top.* 63 (2001) 016310.